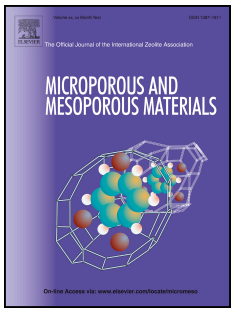
Accepted Manuscript



Bentonite/carbon composite as highly recyclable adsorbents for alkaline wastewater treatment and organic dye removal

Xiaoyu Liang, Yi Lu, Zhijuan Li, Chao Yang, Chunge Niu, Xintai Su

PII: S1387-1811(16)30575-3

DOI: 10.1016/j.micromeso.2016.12.016

Reference: MICMAT 8045

To appear in: *Microporous and Mesoporous Materials*

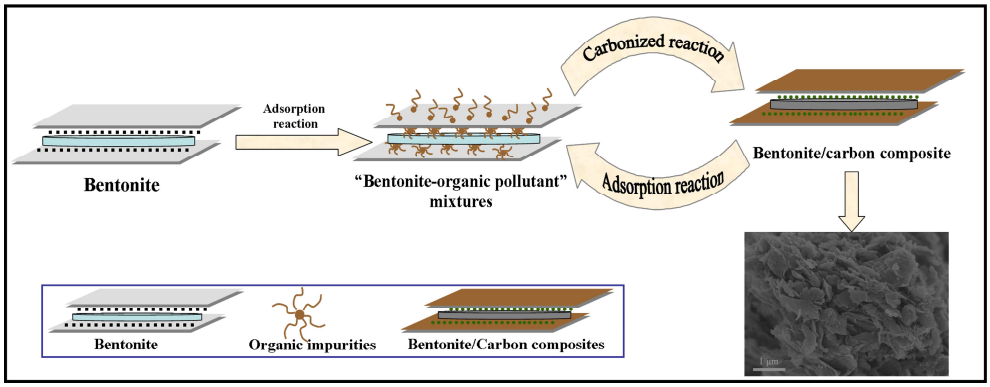
Received Date: 26 October 2016

Revised Date: 5 December 2016

Accepted Date: 10 December 2016

Please cite this article as: X. Liang, Y. Lu, Z. Li, C. Yang, C. Niu, X. Su, Bentonite/carbon composite as highly recyclable adsorbents for alkaline wastewater treatment and organic dye removal, *Microporous and Mesoporous Materials* (2017), doi: 10.1016/j.micromeso.2016.12.016.

This is a PDF file of an unedited manuscript that has been accepted for publication. As a service to our customers we are providing this early version of the manuscript. The manuscript will undergo copyediting, typesetting, and review of the resulting proof before it is published in its final form. Please note that during the production process errors may be discovered which could affect the content, and all legal disclaimers that apply to the journal pertain.



ACCEPTED MANUSCRIPT

ACCEPTED MANUSCRIPT

Bentonite/carbon composite as highly recyclable adsorbents for alkaline wastewater treatment and organic dye removal

Xiaoyu Liang, Yi Lu, Zhijuan Li, Chao Yang, Chunge Niu, Xintai Su*

Ministry Key Laboratory of Oil and Gas Fine Chemicals, College of Chemistry and Chemical Engineering, Xinjiang University, Urumqi 830046, China

Abstract

Alkaline wastewater is high-concentrated and refractory organic wastewater from oil refinery, and its chemical oxygen demand (COD) ranged from tens of thousands to more than 100,000 $mg \cdot L^{-1}$. This kind of wastewater is very difficult to deal with. In this study, natural bentonite (BT) was used as the adsorbent to treat the alkaline wastewater. Subsequently, the used BT containing numerous organic compounds was calcined in inert atmosphere to prepare BT/carbon composite (BTCC). This adsorption-calcinations process can be repeated for 9 times and the adsorption performance does not decrease. The characterization results confirmed that as-prepared BTCC has irregular flake-shaped structures, and the carbon content of samples was increased with increased recycle. The adsorbents can be recycled to deal with alkaline wastewater and reduce the COD value of alkaline wastewater. The percentage removal of COD was 91% after recycling 9 times. Moreover, the recycling BTCC also showed superior adsorption behavior for methylene blue (MB). The equilibrium adsorption isotherms were better fitted by the Freundlich isotherm, and the kinetics model of MB adsorption was ideally conformed to pseudo-second-order model. This process realized the principle of “using waste to treat waste”, and obtained excellent recyclable adsorbent material for organic wastewater treatment.

Key words: Bentonite/carbon composite; Recycle; COD; Methylene blue; The adsorption capacity.

ACCEPTED MANUSCRIPT

1. Introduction

The new era of modern world is facing many environmental problems like overflowing landfills, water scarcity, climate change, water and air pollution etc. [1]. Meanwhile, the demand for implementation of efficient treatment technologies is increasing and various methods have been developed for wastewater treatment such as chemical oxidation, coagulation, precipitation, ozonation, biological treatment and adsorption process [2-5]. Among them, adsorption technology as a simple, rapid and reliable method has been widely used in removal of organic contaminants from wastewater [5-8].

Different adsorbents have been developed by researchers for the removal of organic waste from water with various degrees of success. On one hand, clay mineral materials have been widely used as a low-cost and sustainable adsorbent, due to their large surface area, high adsorptive property and ion exchange ability. As a member of the clay group, bentonite (BT) is a kind of layered silicate clay mineral and composed primarily of montmorillonite. It has been widely employed as adsorbent on some industrial application [9-12]. However, it is always rapidly deactivated after adsorption, due to deposition of various organics on the surface. The regeneration of BT often requires tedious steps and high cost [13, 14]. On the other hand, various carbon materials, including activated carbon [7, 15, 16], carbon aerogel [17-19], templated carbon [20, 21], carbon nanotube [22-25], and even graphene [26, 27], often contain pores with variable range and have been extensively explored as the adsorbents for water-treatment.

Recently, much attention has been paid for the development of clay/carbon composite materials and for their use in a wide variety of applications [1, 28, 29]. Because they were claimed to exhibit improved properties such as recycle ability, adsorption, swelling and ion exchange properties. Considering the benefits of clay/carbon composites, research on the preparation of them has been performed in the last decades. For instance, Yamamoto et al. [30, 31] prepared clay-carbon composite by sintering the mixtures of clay and porous carbon. The obtained composite showed large surface area, high porosity and good electrical conductivity. Yates research groups [32] prepared carbon-clay composites by the introduction of a silicate clay binder and a commercially available activated carbon for effluent decontamination. Ruiz-Hitzky and his coworkers [33, 34] also had prepared a series of carbon-clay composites by using caramel or sucrose as carbon source and phyllosilicates or sepiolite as clay minerals. Despite considerable recent progress on the clay/carbon composites, it is still desired to develop a facile and low-cost method to prepare carbon-clay composites [35, 36].

Alkaline wastewater is a high-concentrated industrial pollutant and contains a very high magnitude of organic waste and is very difficult to deal with. In this study, a highly recyclable bentonite/carbon composite (BTCC) adsorbent was prepared by treating the alkaline wastewater with BT together with a subsequent calcinations process. The purpose of this process was attempt to use the principle of “using waste to treat waste” and obtained an excellent adsorption material for organic wastewater treatment, and showed a potential application in environmental protection industry.

2. Materials and methods

2.1 Materials

The alkaline wastewater used in this study was supplied by oil refinery of the Dushanzi (China); the characteristics of major raw wastewater are reported in Table 1. The basic dyes used as adsorbate is cationic dye methylene blue (MB), which was purchased from Tianjin Bodi Chemical Reagent Company (China). BT employed as adsorbent in the present study was purchased from Xiazijie (China) and its abbreviation is X-Na-BT. All the reagents used in this experiment are analytical grade.

2.2 Preparation of the composite adsorbents

First, the alkaline wastewater was filtered through wire gauze to remove suspended solids. Second, the pH was first adjusted to 2 with HCl (6 M) and then adjusted to 9 with NaOH (2 M) before chemical oxidation process [37, 38]. The adsorption tests were carried out by agitating 100 mL of wastewater with 5 g of X-Na-BT adsorbent under ultrasonic vibration for 2 h. After the reaction was completed, the emulsion-like mixtures were separated by centrifugation at 2500 rpm for 10 min. The chemical oxygen demand (COD) value of supernatant was related to the total concentration of organics (such as: naphthenic acid salt, free alkali, phenol compounds) and determined by potassium dichromate oxidation process. The COD value was calculated by the following equation (1):

$$\text{COD value} = (V_0\text{-}V_1)\ c*8*1000/V \quad (1)$$

Where c (mol/L) is the concentration of $(NH_4)_2Fe(SO_4)_2\cdot 6H_2O$ solution, V_0 (mL) is the volume value of $(NH_4)_2Fe(SO_4)_2\cdot 6H_2O$ consumed by sample solution, V_1 (mL) is the volume of $(NH_4)_2Fe(SO_4)_2\cdot 6H_2O$ consumed by the water, and V (mL) the volume value

of sample solution. 8 (g/mol) denotes the molar mass of oxygen (1/2 O) and 1000 is volume unit conversion factor.

Then the bottom adsorbent containing organic impurities was dried at 80^{o}C for 24 h. The dry solid was carbonized in Ar atmosphere at a heating rate of 5^{o}C·min^{-1} to 500^{o}C and maintained at this temperature for 2 h, and then the BT/carbon composite was obtained. Furthermore, the experiments at the same conditions were repeated 8 times using the carbonized composite adsorbents, as schematically illustrated in Fig. 1. COD removal efficiency was defined as follows:

$$\text{COD removal efficiency (\%)} = (COD_0 - COD_f)/COD_0 * 100 \cdots\cdots\cdots\cdots\cdots\cdots (2)$$

Where COD_0 and COD_f are the initial and final chemical oxygen demands, respectively. Then the results were depicted in Table 2. All the ultrasonic processes were done in a water bath ultrasonic cleaning machine.

2.3 Characterization of the adsorbents

The Brunauer-Emmett-Teller (BET) surface area, pore volume and pore size distribution were determined by nitrogen adsorption/desorption isotherm technique. The chemical compositions of adsorbents were characterized by field-emission scanning electron microscopy (FESEM) in a Hitachi SU8010 microscope coupled with a Link energy-dispersive spectroscopy (EDS) analytical microprobe for element identification. Raman spectra were measured by Bluker Senterra with 532 nm wavelength laser source. In order to detect the functional groups of the samples, Fourier transform infrared (FTIR) spectra were recorder on a Bruker-EXUINOX55 spectrometer. The adsorption performance was recorded with a UV-vis absorption spectrum (Shimadzu, model

UV-2550, Tokyo).

2.4 Adsorption studies

MB is a water-soluble cationic dye commonly used in textile industry. It was selected as a simulated organic wastewater to investigate the adsorption properties of the samples [39]. The adsorption process was performed as the following procedure described. 10 mg of adsorbent was added to 100 mL of MB solution (20 $mg \cdot L^{-1}$) and the mixture was agitated at 160 rpm and 25^{o}C in a rotary shaker. Then the adsorbents were separated through centrifugation at different time intervals (0, 1, 5, 15, 25, 45, 65 min) and the concentration of MB in the supernatants was examined by a UV-vis spectrophotometer at the λ_{max} = 664 nm. To evaluate the adsorption capacity, 10 mg of adsorbent was dispersed into 20 mL of MB solution with different initial concentrations (20-300 $mg \cdot L^{-1}$). After stirring at room temperature for 12 h in the dark, the solutions were centrifuged at 2500 rpm and the residual MB concentration in the supernatants was estimated by monitoring the absorbance at the λ_{max} = 664 nm. Then the amounts of MB adsorbed per unit mass of adsorbent were calculated from the differences between the initial and final MB concentrations in solution by the following equation (3):

$$q_t = (C_0 - C_t)\ V/W \quad \cdots\cdots\cdots\cdots\cdots\cdots\cdots\cdots\cdots\cdots\cdots\cdots\cdots\cdots \quad (3)$$

Here q_t ($mg \cdot g^{-1}$) was the adsorption capacity at any time t (min). C_0 and C_t ($mg \cdot L^{-1}$) were the initial and final concentrations of MB solution, respectively. V (L) was the volume of MB solution used, and W (g) was the mass of the adsorbent used in the present study.

3. Results and discussion

3.1 COD removal of alkaline wastewater

The experiments were carried out according to the proposed experimental design. The initial characteristics of the wastewater are presented in Table 1. The results monitored by potassium dichromate oxidation method were presented in Table 2 and the related histogram was drawn in Fig. 2. It can be found that the removal efficiency of COD was 67.1% (X-Na-BT). Then X-Na-BT adsorbed alkaline wastewater was known as “BT-organic pollutant” mixtures. The “BT-organic pollutant” mixtures were calcined to produce recycled BT/carbon composite material (referred to as BTCC). After the first adsorption-calcinations, the COD removal efficiency reached 97.2%, as shown in Table 2 and Fig. 2. After that, the COD removal efficiency was decreased with increase in cycle number, namely from 97.2% (the 2nd cycle) to 58.8% (the 7th cycle). Then the COD removal value was enhanced to near 90.6% after recycled 9 times. These result clearly revealed that the BTCC can be recycled at least 9 times and served as an efficient absorbent for the purification of wastewater.

According the experiment results and previous reports, we propose a synergistic adsorption mechanism [40]. It is known that carbon materials such as active carbon or mesoporous carbon can be used as adsorbents [41]. With the increase of cyclic adsorption-carbonization times, the carbon content of the composite was gradually increased, and the adsorption capacity was maintained at a high numerical value. Second, carbon may play a synergistic role in the BT/carbon composite. The size of the surface mesopores increased with increasing carbon content. Smaller molecules can access but would be extremely easy to escape from the pores or larger molecules cannot

access the pores, even when there are multiple contact points between the adsorbate and adsorbent, resulting in the adsorption of alkaline wastewater being restricted.

3.2 Characterization

3.2.1 Physical adsorbent characterization

The surface areas and pore structure of the adsorbents were determined by N_2 adsorption/desorption analysis, and the results are displayed in Table 3, together with Fig. 3. As can be seen from Table 3, the surface area, pore volume and average pore size were increased from X-Na-BT to BTCC-8, which was consistent with the increasing level of carbonization. The size of the mesopores is defined as 2-50 nm in diameter. The pore size distribution (Fig. 3) in the range of 2-10 nm was analyzed using the desorption branch of the isotherm. The results illustrated that the samples consisted mostly of mesopores, with a pore size range of 2-4 nm. These results are consistent with the assumption of the results of Fig. 2.

3.2.2 FESEM and the corresponding EDS analyses of the samples

The morphology of samples was investigated by FESEM and shown in Fig. 4. It can be obviously seen from Fig. 4a that sample had obvious curly layered structures. After the carbonization process, its surface morphology did not change significantly, but the carbon content of the composite was gradually increased along with the increase of cycle number (Fig. 4(b-d)). The BTCC sorbent exhibited a slightly rough surface (Fig. 4(b2, c2, and d2)), while a smooth morphology was observed on the surface of X-Na-BT sorbent (Fig. 4(a2)), which indicated that the pyrolysis of organic impurities caused the formation of rough surface [42].

3.2.3 Raman analyses of the samples

To get information on the structure of carbon loaded on BT, the samples were characterized by the Raman spectroscopy. The Raman spectra are shown in Fig. 5. Two typical first order bands appear, i.e. the G band (located at about 1580 cm^{-1}) and the D band (at around 1340 cm^{-1}). From the Raman spectra one can also see that the spectrum has been shifted in the vertical direction. The D peak has a wavenumber shift of approximately 100 cm^{-1}. But the peak position of the G band increases with an increase of cycle number, in terms of wavenumber shift. This might be due to the change in the size of the samples and the band gap. Secondly, changes in the peak position may also be related to the changes in the inter-atomic forces and the equilibrium positions of the lattice change [43]. The results indicated that the framework of carbon sheets became a more graphitized carbon [44].

3.2.4 FTIR analyses of the samples

FTIR spectra can reveal the surface functional groups on carbon's surface, although some particular peaks overlap might exist [7]. Fig. 6 shows the FTIR spectra of X-Na-BT and BTCC. The characteristic vibration bands of X-Na-BT were detectable at 3628 cm^{-1}, which was recognized to be O-H stretching mode in molecular water and Si-OH. In addition, peaks around 3413 cm^{-1} and 1643 cm^{-1} were corresponded to the angular and axial deformations of the hydration water, respectively [45]. As seen in Fig. 6, the characteristic adsorption bands of BT appeared at 1039, 798, 623 and 522 cm^{-1} which can be assigned to Si-O stretching peaks in SiO_4^- tetrahedral. Meanwhile, the intensity of characteristic peaks of BT at 3628 and 1640 cm^{-1} were significantly reduced,

which was due to the increased carbon content after repeating adsorption-calcinations experiments (Fig. 6(b-d)) [46]. The band was also observed in the region between 1400 and 1500 cm^{-1} after 9th cycle number (Fig. 6d), which implied the formation of carbon during the calcinations process.

3.3 Adsorptive properties for MB

3.3.1 Adsorption rate and adsorption capacity

In order to explain the adsorption behavior of as-prepared samples, a comparative study was implemented under the same experimental conditions. In the present work, X-Na-BT and BTCC-1 were used as the adsorbents for MB removal. The adsorption of MB onto the adsorbents was investigated at different times and different concentrations, and the results are listed in Fig. 7. Fig. 7(a, c) indicated the temporal evolution of absorption spectra of MB solution in the presence of the adsorbents. The adsorption peak intensity corresponding to the MB molecules at 664 nm diminishes sharply and even disappears compared to the initial MB solution after treatment for about 25 min. It can also be clearly seen from the inset in Fig. 7(a, c) that the MB adsorption increased with an increase in contact time. The adsorption rate was very high in the first 1 min, and reached equilibrium in 45 min. We attributed the rapid equilibrium process to the high diffusion of the dye molecules into the external surface of the samples or the boundary diffusion layer of the solute molecules [47]. At later times the available adsorption sites became fewer, which decreased the adsorption capacity and an equilibrium state was achieved [48]. Fig. 7(b, d) showed the relation between the adsorption capacities of the adsorbents and the initial concentrations of MB. It could be

observed that the adsorption capacities of the adsorbents increased with increase in the initial MB concentration. The equilibrium adsorption capacity of MB onto X-Na-BT and BTCC-1 were 288.9 and 270.1 $mg\cdot g^{-1}$, respectively.

3.3.2 Adsorption isotherms

In order to give a deeper analysis on the adsorption properties, adsorption isotherms are available to study how the adsorbate molecules are distributing between the solid and liquid phases at certain temperature. Langmuir and Freundlich isotherm models were adopted to portray the relationship between equilibrium concentration and the amount of MB adsorbed on the adsorbents.

The Langmuir isotherm model is applicable to homogeneous sorption, and predicts the maximum monolayer adsorption capacity of the adsorbent. The expression of the Langmuir equation is shown in equation (4):

$$q_e = q_m K_L C_e / (K_L C_e + 1) \quad \cdots\cdots (4)$$

Where q_e ($mg\cdot g^{-1}$) is the adsorption capacity of the adsorbent at equilibrium, and C_e ($mg\cdot L^{-1}$) is the adsorbate concentration at equilibrium time; q_m ($mg\cdot g^{-1}$) is the maximum monolayer adsorbent capacity; K_L ($L\cdot mg^{-1}$) is the Langmuir constant; q_m and K_L are obtained from the intercept and slope of linear plot of $C_e\ q_e^{-1}$ versus C_e, respectively and are shown in Table 4.

The Freundlich isotherm is usually employed for multilayer adsorption on a heterogeneous adsorbent surface. The non-linear expression of the Freundlich model is reported in equation (5):

$$q_e = K_F C_e^{1/n} \quad \cdots\cdots (5)$$

Where K_F is the Freundlich constant related to the adsorption capacity of the adsorbents, and 1/n is the reciprocal of reaction order which is a function of the strength of adsorption.

The isotherm curves based on the experimental data and the correlations by both models are provided in Fig. 8. The calculated values of Langmuir and Freundlich model's parameters are presented in Table 4 [49]. According to the comparison of the correlation coefficient values (R^2), the Freundlich isotherm model yielded a much better fit than the Langmuir model for study adsorption from aqueous solutions. Furthermore, the values of *n* at equilibrium were bigger than 1, indicated that the MB adsorption onto the adsorbents was favorable under the experimental condition. In addition, the Freundlich constant K_F was indicative of the adsorption capacity of the adsorbent (see Table 4). It is supposed that BTCC-1 (K_F = 5.49) may have a stronger adsorption capacity for MB in the solution than X-Na-BT (K_F = 4.39). These results revealed that the Freundlich model can better describe an adsorption isotherm for X-Na-BT and BTCC-1. This adsorptive behavior indicated that the adsorption may take place on heterogeneous surfaces of adsorbents, which may be attributed to the various active sites on adsorbents having different affinities to MB molecules.

3.3.3 Adsorption kinetic studies

In order to investigate the controlling mechanism of adsorption processes such as mass transfer and chemical reaction, kinetic models were used to test experimental data. The kinetics of MB adsorption onto X-Na-BT and BTCC-1 was analyzed using pseudo-first-order and pseudo-second-order kinetics models. The pseudo-first-order

kinetic model can be expressed as:

$$\lg(q_e - q_t) = \lg q_e - K_1 t/2.303 \cdots\cdots (6)$$

Where q_e and q_t ($mg \cdot g^{-1}$) are the amounts of MB adsorbed at equilibrium and at time t, respectively, and K_1 (min^{-1}) is the rate constant for pseudo-first-order adsorption. The values of rate constant can be obtained from the slope of the plot of $\lg(q_e-q_t)$ versus t.

The pseudo-second-order kinetic model is expressed as:

$$t/q_t = 1/(K_2 q_e^2) + t/q_e \cdots\cdots (7)$$

Where K_2 ($g \cdot mg^{-1} \cdot min^{-1}$) is the rate constant of the pseudo-second-order adsorption. K_2 and q_e were determined from the intercept and slope of the plot t/q_t versus t and there was no need to know any parameter beforehand.

The kinetic models with the equilibrium adsorption capacities of the samples are illustrated in Fig. 9 and the calculated parameters from the fitted kinetic models are given in Table 5. From Fig. 9a, it can be seen that the first order kinetic curves of all adsorbents didn't give a straight line but showed a clear identification into several regions. The low correlation coefficients (R^2 values; see Fig. 9a and Table 5) indicated that adsorption of MB onto these adsorbents did not follow a first-order model. On the contrary, the fitted linear regression plot indicated that the experimental data were well fitted to the pseudo-second-order kinetics model with the extremely high $R^2 > 0.99$ (Fig. 9b; Table 5). The conclusion drawn from the experimental data revealed that the sorption followed pseudo-second-order kinetics, the adsorption mechanism depended on the adsorbate as well as adsorbent, and the rate-limiting step may be chemisorptions involving valence forces through sharing or exchange of electrons [50].

4. Conclusions

This process attempts to put into use the principle of “using waste to treat waste”. BT was used as adsorbent for alkaline wastewater treatment. The used BT containing organic compounds can be recycled by a facile calcinations process under Ar atmosphere to obtain BTCC. The obtained composites were recycled to deal with organic alkaline wastewater for many times without a significant decrease in its adsorption performance. The COD removal percentage of alkaline wastewater can be as high as 91% after recycling 9 times. Meanwhile, they can also use for MB adsorption. The equilibrium adsorption isotherms studies revealed that the Freundlich isotherm model satisfactorily described the sorption data, and the equilibrium adsorption capacity were up to 287.0 $mg \cdot g^{-1}$ (X-Na-BT) and 270.1 $mg \cdot g^{-1}$ (BTCC-1), respectively. The kinetics model of MB adsorption onto X-Na-BT and BTCC-1 suggested that adsorption profiles followed pseudo-second-order model. The results of this work demonstrate that the highly recyclable BTCC adsorbents can be used as a promising candidate for wastewater treatment.

Acknowledgments

This work was supported by the National Natural Science Foundation of China (51174174), Project of Xinjiang Province (201491127) and Excellent Doctor Innovation Program of Xinjiang University (No. XJUBSCX-2014010).

References

[1] M. Nafees, A. Waseem, Clean-Soil, Air, Water. 42 (2014) 1500-1508.
[2] Z. Aksu, J. Yener, Waste Manage. 21 (2001) 695-702.
[3] F. Banat, S. Al-Asheh, L. Al-Makhadmeh, Chem. Eng. Technol. 27 (2004) 80-86.
[4] A.R. Mermut, G. Lagaly, Clay. Clay Miner. 49 (2001) 393-397.

[5] Y. Bulut, H. Karaer, Chem. Eng. Commun. 202 (2015) 1635-1644.
[6] M. Rafatullah, O. Sulaiman, R. Hashim, A. Ahmad, J. Hazard. Mater. 177 (2010) 70-80.
[7] E.K. Putra, R. Pranowo, J. Sunarso, N. Indraswati, S. Ismadji, Water Res. 43 (2009) 2419-2430.
[8] C. Nie, Z. Peng, Y. Yang, C. Cheng, L. Ma, C. Zhao, J. Hazard. Mater. (2016).
[9] W.W. Ngah, L. Teong, M. Hanafiah, Carbohydr. Polym. 83 (2011) 1446-1456.
[10] V. Srivastava, C. Weng, V. Singh, Y. Sharma, J. Chem. Eng. Data. 56 (2011) 1414-1422.
[11] C. Zhou, Q. Wu, T. Lei, I.I. Negulescu, Chem. Eng. J. 251 (2014) 17-24.
[12] L. Obeid, N. El Kolli, N. Dali, D. Talbot, S. Abramson, M. Welschbillig, V. Cabuil, A. Bée, J. Colloid Interface Sci. 432 (2014) 182-189.
[13] M. Bansal, U. Garg, D. Singh, V. Garg, J. Hazard. Mater. 162 (2009) 312-320.
[14] P.-L. Boey, S. Ganesan, G.P. Maniam, D.M.H. Ali, Energy Convers. Manage. 52 (2011) 2081-2084.
[15] D. Nguyen-Thanh, T.J. Bandosz, Carbon. 43 (2005) 359-367.
[16] K.L. Wasewar, P. Kumar, S. Chand, B.N. Padmini, T.T. Teng, Clean-Soil, Air, Water. 38 (2010) 649-656.
[17] A.K. Meena, G. Mishra, P. Rai, C. Rajagopal, P. Nagar, J. Hazard. Mater. 122 (2005) 161-170.
[18] W. Chen, X. Yang, J. Huang, Y. Zhu, Y. Zhou, Y. Yao, C. Li, Electrochim. Acta. 200 (2016) 75-83.
[19] E. Hu, X. Wu, S. Shang, X.M. Tao, S.X. Jiang, L. Gan, J. Clean. Prod. 112 (2016) 4710-4718.
[20] C. González-Gaitán, R. Ruiz-Rosas, H. Nishihara, T. Kyotani, E. Morallón, D. Cazorla-Amorós, Carbon. 99 (2016) 157-166.
[21] G. Rasines, P. Lavela, C. Macías, M. Haro, C. Ania, J. Tirado, J. Electroanal. Chem. 671 (2012) 92-98.
[22] Y. Li, W. Zhou, H. Wang, L. Xie, Y. Liang, F. Wei, J.-C. Idrobo, S.J. Pennycook, H. Dai, Nat. Nanotechnol. 7 (2012) 394-400.
[23] X. Liu, M. Wang, S. Zhang, B. Pan, J. Environ. Sci. 25 (2013) 1263-1280.
[24] B. Lee, Y. Baek, M. Lee, D.H. Jeong, H.H. Lee, J. Yoon, Y.H. Kim, Nat. Commun. 6 (2015).
[25] N. Konikkara, L.J. Kennedy, J.J. Vijaya, J. Hazard. Mater. 318 (2016) 173-185.
[26] K. Goh, L. Setiawan, L. Wei, R. Si, A.G. Fane, R. Wang, Y. Chen, J. Membr. Sci. 474 (2015) 244-253.
[27] C. Ruiz-García, M. Darder, P. Aranda, E. Ruiz-Hitzky, J. Mater. Chem. A. 2 (2014) 2009-2017.
[28] A.S. Bhatt, P.L. Sakaria, M. Vasudevan, R.R. Pawar, N. Sudheesh, H.C. Bajaj, H.M. Mody, RSC Adv. 2 (2012) 8663-8671.
[29] Y. Zhou, X.-Y. Jin, H. Lin, Z.-L. Chen, Chem. Eng. J. 166 (2011) 176-183.
[30] T. Kanbara, T. Yamamoto, H. Ikawa, T. Tagawa, H. Imai, J. Mater. Sci. 24 (1989) 1552-1558.
[31] T. Yamamoto, T. Kanbara, Inorg. Chim. Acta. 142 (1988) 191-193.
[32] M. Yates, M. Martín-Luengo, L.V. Argomaniz, S.N. Velasco, Micropor. Mesopor. Mat. 154 (2012) 87-92.
[33] M. Darder, E. Ruiz-Hitzky, J. Mater. Chem. 15 (2005) 3913-3918.
[34] A. Gómez-Avilés, M. Darder, P. Aranda, E. Ruiz-Hitzky, Angew. Chem. Int. Edit. 46 (2007) 923-925.
[35] G.A. Ahmed I, Appl. Energ. 86 (2009) 1813-1821.
[36] A. Redding, S. Burns, R. Upson, E. Anderson, J. Colloid Interf. Sci. 250 (2002) 261-264.
[37] S.I. Abou-Elela, M.E.M. Ali, H.S. Ibrahim, Arab. J. Chem. (2014).
[38] G. Pliego, J.A. Zazo, J.A. Casas, J.J. Rodriguez, J. Hazard. Mater. 252 (2013) 180-185.
[39] C. Namasivayam, D. Kavitha, Dyes. Pigments. 54 (2002) 47-58.
[40] L.H. Torn, A. de Keizer, L.K. Koopal, J. Lyklema, J. Colloid Interf. Sci. 260 (2003) 1-8.

ACCEPTED MANUSCRIPT

[41] B. Gao, P.S. Yap, T.M. Lim, T.-T. Lim, Chem. Eng. J. 171 (2011) 1098-1107.

[42] H. Alves, A. da Rocha, M. Monteiro, C. Moretti, M. Cabrelon, C. Schwengber, M. Milinsk, Appl. Clay Sci. 91 (2014) 98-104.

[43] L. Li, B. Suen, F.E. Talke, IEEE T. Magn. 51 (2015).

[44] S. Tanaka, T. Yasuda, Y. Katayama, Y. Miyake, J. Membrane Sci. 379 (2011) 52-59.

[45] L. Cótica, V. Freitas, I. Santos, M. Barabach, F. Anaissi, R. Miyahara, P. Sarvezuk, Appl. Clay Sci. 51 (2011) 187-191.

[46] J. Martín-Alfonso, C. Valencia, J. Franco, Appl. Clay Sci. 87 (2014) 265-271.

[47] F.S. Hashem, Hydrol Current Res 3:143, Page 2 of 6, Volume 3, Issue 5, 2012.

[48] M. Pooresmaeil, Y. Mansoori, M. Mirzaeinejad, A. Khodayari, Adv. Polym. Tech. (2016).

[49] L. Zhu, L. Zhang, Y. Tang, D. Ma, J. Yang, J. Elastom. Plast. 47 (2015) 488-501.

[50] O. Eljamal, J. Okawauchi, K. Hiramatsu, M. Harada, Environ. Earth Sci. 68 (2013) 859-863.

ACCEPTED MANUSCRIPT

Tables:

Table 1. Typical raw wastewater characteristics (all values except pH are in mg/L).

Parameter	pH	VP	COD	TDS	Chromaticity	TAN
Values	13.4	600	79834	20000	15000	3557

Notes: VP—volatile phenol; COD—chemical oxygen demand; TDS—total dissolved solids; TAN—total ammonia-nitrogen.

ACCEPTED MANUSCRIPT

Table 2. Variation of the COD value after the adsorption treatment.

Adsorbent	Ultrasonic time	COD removal values (mg/L)
X-Na-BT	2 h	53569
BTCC-1	2 h	77599
BTCC-2	2 h	67300
BTCC-3	2 h	57001
BTCC-4	2 h	55564
BTCC-5	2 h	48459
BTCC-6	2 h	46942
BTCC-7	2 h	53808
BTCC-8	2 h	72330

Note: the superscript number (1-8) represents the cycle number.

ACCEPTED MANUSCRIPT

Table 3. Textural properties of different adsorbents.

Adsorbent	S_{BET} (m^2/g)	D_{ave} (nm)	V_{Total} (cm^3/g)
X-Na-BT	15.6	2.61	0.012
BTCC-1	23.3	2.81	0.041
BTCC-6	18.9	2.73	0.030
BTCC-8	27.6	2.85	0.048

Note: D_{ave}---average pore diameter; V_{Total}---total pore volume.

ACCEPTED MANUSCRIPT

Table 4. Parameters of Langmuir and Freundlich isothermal adsorption equation.

Adsorbent	Langmuir adsorption				Freundlich adsorption		
	q_m	K_L	R^2	R_L	K_F	n	R^2
X-Na-BT	543.5	4.88×10^{-3}	0.7630	0.406	4.39	1.27	0.9181
BTCC-1	448.4	6.21×10^{-3}	0.8794	0.349	5.49	1.37	0.9163

ACCEPTED MANUSCRIPT

Table 5. Kinetic constant parameters obtained for the adsorption of MB onto the adsorbents.

Adsorbent	Pseudo-first-order			Pseudo-second-order		
	q_e	K_1	R^2	q_e	K_2	R^2
X-Na-BT	7.83	0.074	0.8354	199.60	0.107	1
BTCC-1	29.18	0.085	0.9366	199.20	0.030	0.99999

ACCEPTED MANUSCRIPT

Figure captions:

Fig. 1 Proposed schematic of fabrication of composite adsorbents.

Fig. 2 The COD removal efficiency of wastewater treated by X-Na-BT and BTCC.

Fig. 3 Pore size distributions of adsorbents.

Fig. 4 FESEM micrographs and the corresponding EDS analysis of (a1-a3) X-Na-BT, (b1-b3) BTCC-1, (c1-c3) BTCC-6, and (d1-d3) BTCC-8.

Fig. 5 Raman spectra of adsorbents BTCC after heating at ~550^{o}C under argon.

Fig. 6 FTIR spectra of the samples: (a) X-Na-BT, (b) BTCC-1, (c) BTCC-6, and (d) BTCC-8.

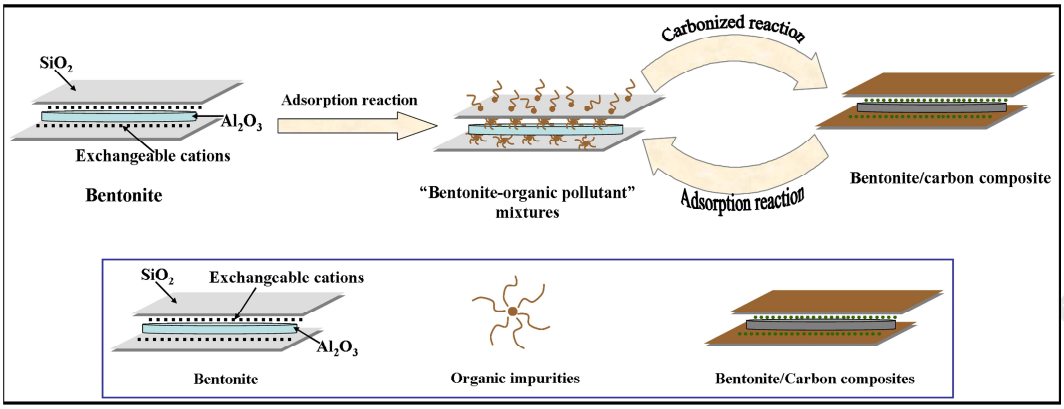
Fig. 7 Adsorption spectrum of MB at different time intervals (inset shows its absorption rate) and adsorption isotherm of MB after treatment with adsorbents (a, b) X-Na-BT, (c, d) BTCC-1.

Fig. 8 Plots of isotherm models for the adsorption of MB onto X-Na-BT and BTCC-1 (a) Langmuir, (b) Freundlich isotherm models.

Fig. 9 Plots of kinetic models for the adsorption of MB on X-Na-BT and BTCC-1 (a) pseudo-first-order, (b) pseudo-second-order kinetics.

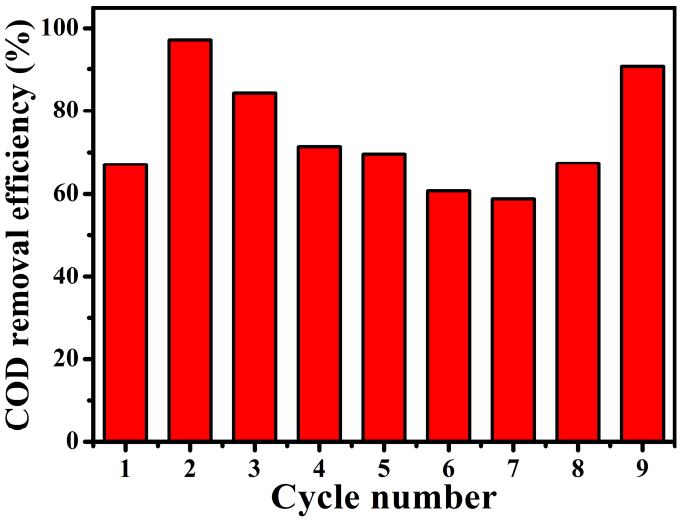
ACCEPTED MANUSCRIPT

ACCEPTED MANUSCRIPT

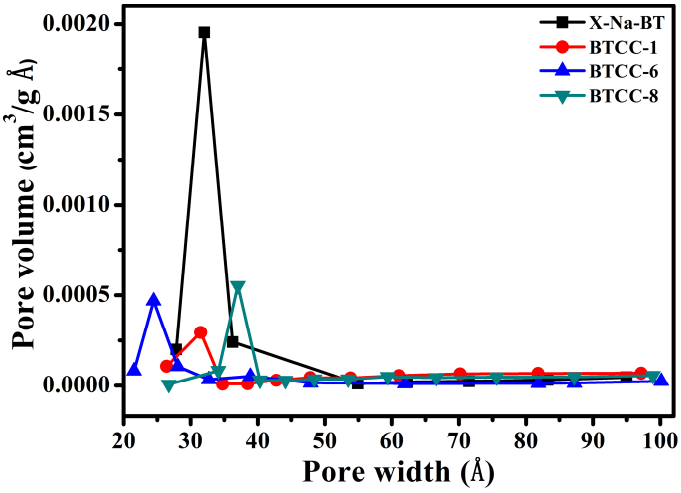


ACCEPTED MANUSCRIPT

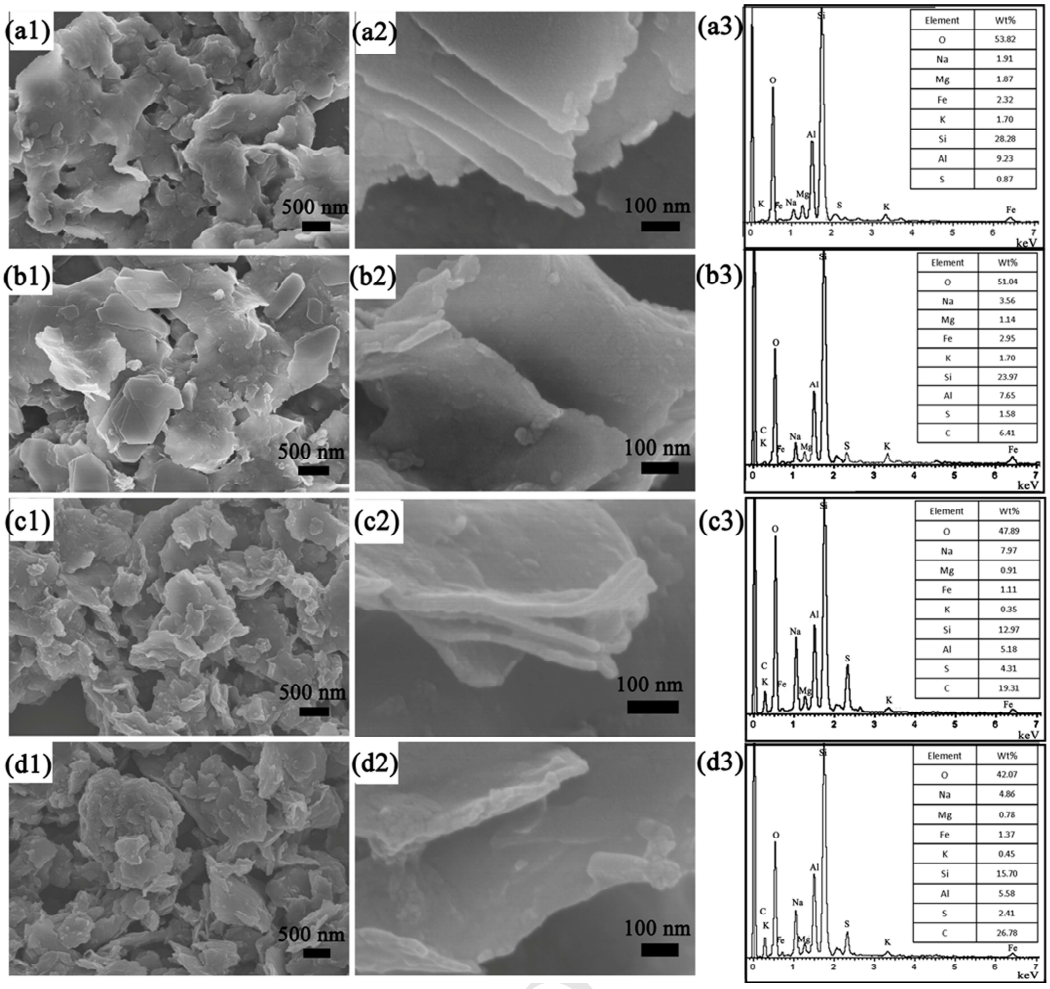
ACCEPTED MANUSCRIPT



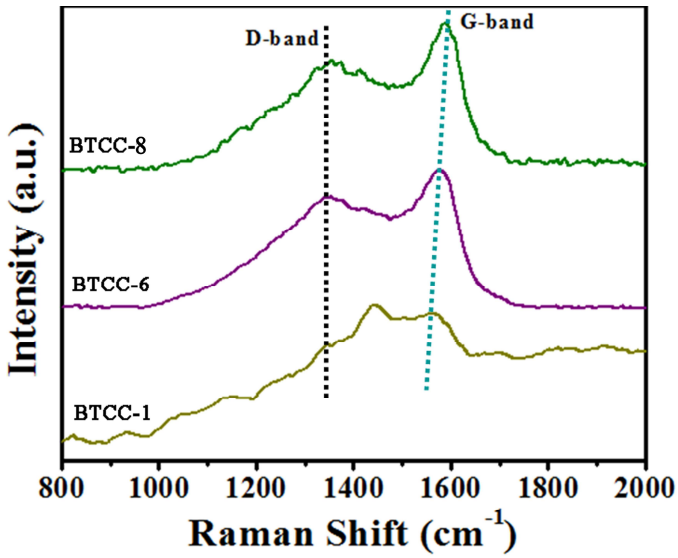
ACCEPTED MANUSCRIPT



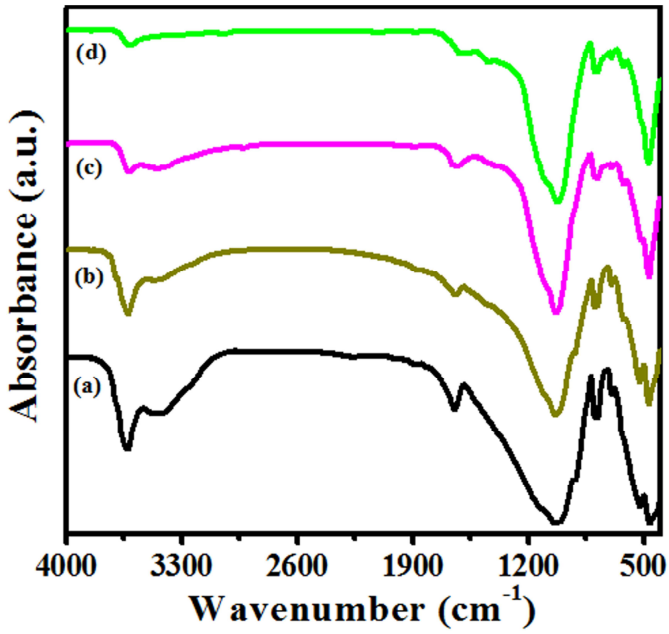
ACCEPTED MANUSCRIPT



ACCEPTED MANUSCRIPT

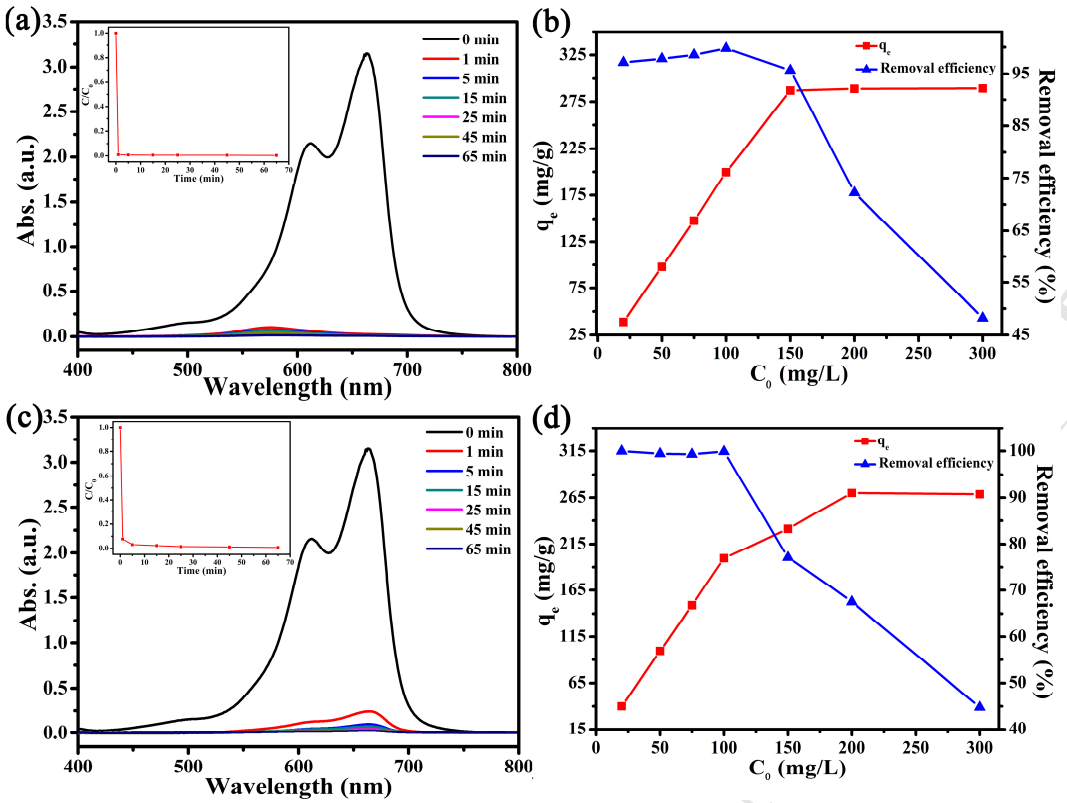


ACCEPTED MANUSCRIPT

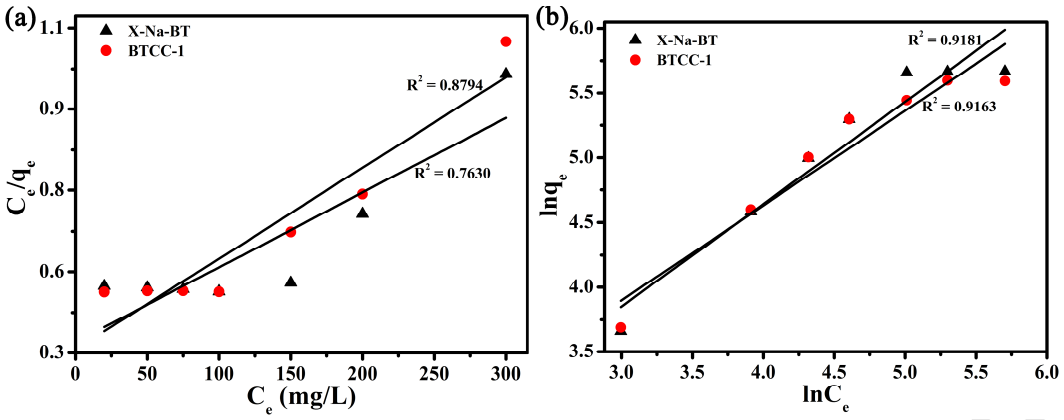


ACCEPTED MANUSCRIPT

ACCEPTED MANUSCRIPT

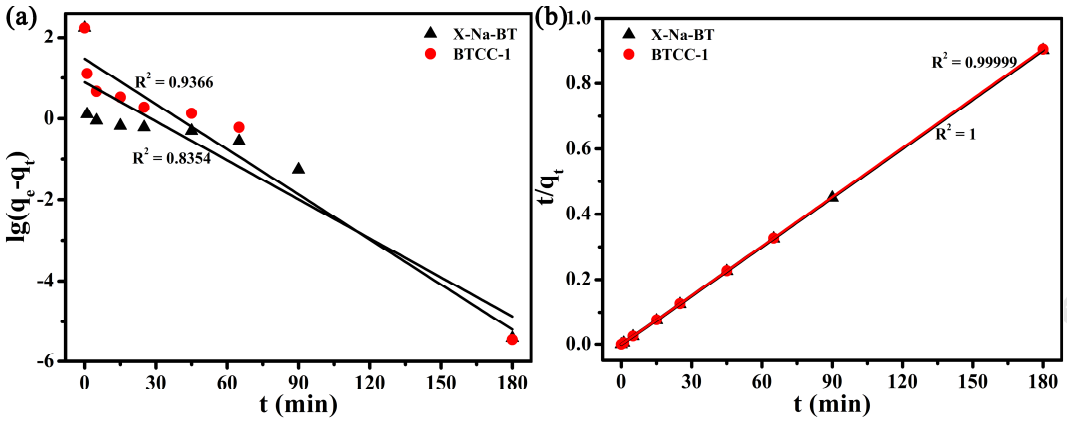


ACCEPTED MANUSCRIPT



ACCEPTED MANUSCRIPT

ACCEPTED MANUSCRIPT



ACCEPTED MANUSCRIPT

ACCEPTED MANUSCRIPT

Highlights

●This process attempts to put into use the principle of “using waste to treat waste”

●An adsorption-calcination process was adopted to prepare bentonite/carbon composites

●The bentonite/carbon composites show a superior adsorption performance for alkaline wastewater

●The bentonite/carbon composites can also be used for methylene blue adsorption.

ACCEPTED MANUSCRIPT